

A Monte Carlo method for overcoming the edge artifacts in MRI-based electrical conductivity mapping

Li Huang¹, Ferdinand Schweser², Karl-Heinz Herrmann², Martin Krämer², Andreas Deistung², and Jürgen Rainer Reichenbach²

¹*in-vivo-MR Group, Faculty 02 (Biology/Chemistry), University Bremen, Bremen, Germany,* ²*Medical Physics Group, Institute of Diagnostic and Interventional Radiology I, Jena University Hospital - Friedrich Schiller University Jena, Jena, Thuringia, Germany*

TARGET AUDIENCE – Researchers interested in algorithmic improvements of MRI-based electrical conductivity mapping.

PURPOSE – Quantitative conductivity mapping (QCM)^{1,2} is a non-invasive MRI-based technique to assess tissue electrical conductivity. Tissue conductivity has been shown to linearly depend on tissue sodium concentration³, thus opening the door for clinical applications like tissue lesion delineation⁴. Furthermore, it provides important input for improving computations of the local specific RF energy absorption rate². QCM is based on the spatial variation of the phase of the complex-valued B_1^+ field, which may be acquired by using, e.g., 3D ultra-short echo time (UTE) sequences^{5,6}. One major limitation of published algorithms for conductivity reconstruction that has hampered clinical application of QCM so far is the presence of partly severe artifacts near tissue interfaces (*edge artifacts*)^{1,7}, which result from the assumption of locally piecewise constant conductivity in the Helmholtz equation². **In this contribution, we present a spatial-domain inversion algorithm for conductivity reconstruction that substantially reduces edge artifacts.** The algorithm is demonstrated both in a dedicated phantom and *in vivo* experiment.

THEORY – The conductivity reconstruction formula under the phase-only assumption² is $\sigma = \Delta\phi/\omega\mu_0$, which indicates that the basis of conductivity reconstruction is the calculation of the local Laplacian of the phase ϕ . One noise-robust implementation is to apply a Gaussian-filtered Laplacian to the phase maps¹. Alternatively, local quadratic fitting method can be applied⁷ with more or less similar results. When the same kernel (Laplacian or quadratic fitting) is used throughout the data, edge artifacts occur at tissue interfaces where the kernel affects tissues with different conductivity. One option is to reduce the size of the fitting kernel near tissue interfaces to reduce edge artefacts⁷. However, small fitting kernels generally result in excessive noise. To overcome this limitation, we propose to use individual fitting kernels for each voxel. We constructed the kernels as follows: *First*, identification of tissue interfaces is achieved based on edges in magnitude images using a 3D image edge detection algorithm⁸. *Then*, in each voxel a Monte-Carlo-based region growing is applied to determine the local region of homogeneous tissue. The resulting fitting kernels have arbitrary shapes and contain a sufficient number of voxels for noise suppression.

METHODS – (1) *Phantom construction* (Fig. 1a): Six cylindrical plastic bottles (diameter: 5 cm, wall thickness: 0.5 mm, height: 7 cm) containing different saline solutions (red labels in Fig. 1a) were placed in a plastic box (size: 35×25×7 cm³). Agar was added to the bottles and background with a concentration of 2.5% (mass fraction) to reduce vibration artifacts during scanning. To investigate the effect of magnetic susceptibility and T_1 variations on the UTE-based measurements of B_1^+ , the bottom row of bottles contained in addition 1 mmol/L of Gd-DTPA (Magnevist, Schering-Plough, Germany), resulting in a susceptibility difference of 0.34 ppm⁹ (which corresponds to the order of magnitude of magnetic susceptibility contrast in human brain⁹) (black labels in Fig. 1a). (2) *Volunteer*: A healthy 60-year-old male was examined. The institutional review board had approved the study before and written informed consent was obtained from the volunteer. (3) *Data acquisition*: An isotropic 3D UTE sequence with a radial “spiky ball” center-out acquisition¹⁰ was applied on a whole-body 3T MRI scanner (Tim Trio, Siemens Medical Solutions, Erlangen, Germany) with a single-channel T_x/R_x double-tuned birdcage coil (³¹P/¹H head coil, Rapid Biomedical, Germany). Parameters for the phantom study: TE 110 μ s, TR 2.9 ms, RF duration 20 μ s, FA 7°, voxel size 1.5³ mm³, 116276 spokes, 2 averages, TA 678 s; for the volunteer study: TE 110 μ s, TR 3.6 ms, RF duration 40 μ s, FA 7°, voxel size 1.125³ mm³, 80492 spokes, 2 averages, TA 584 s. (4) *Computing server*: A standard PC with a CPU of Intel® Xeon® E5520 (2.27 GHz, 8 cores) and 24 GB RAM was used. (5) *Data pre-processing*: UTE phase images were reconstructed from raw MR data¹¹, unwrapped¹² and divided by two according to the transceiver phase assumption². (6) *Analysis*: Edge artifacts in conductivity maps reconstructed by the Gaussian-filtered Laplacian calculus and the novel Monte Carlo method were compared. Mean conductivities and standard deviations (STD) were calculated in the bottles and background of the phantom (central slices) and in white matter of the brain and compared to previously reported conductivity values (model of saline conductivity¹³ and study of tissue dielectric properties¹⁴).

RESULTS – (1) *Phantom experiment*: Compared to the conductivity maps reconstructed with the Gaussian-filtered Laplacian calculus (duration: 1 min, Fig. 1b), the conductivity maps reconstructed with the novel Monte Carlo method (duration: 25 min, Fig. 1c) show substantially decreased edge artifacts near the bottles’ walls without sacrificing homogeneity in the bottles. The conductivities of the bottles with and without Gd-DTPA are plotted in Fig. 1d (red and blue dots with error bars for Gaussian-filtered Laplacian calculus and yellow and green dots with error bars for novel Monte Carlo method, respectively) as a function of concentration. The values approximately coincided and were also in good agreement with literature¹³ (Fig. 1d, black line), suggesting that susceptibility differences in the bio-physiological range do not affect UTE-based QCM. The STDs were all below 0.2 S/m, reflecting effective noise suppression. (2) *Volunteer experiment*: Compared to the conductivity map reconstructed with the Gaussian-filtered Laplacian calculus (duration: 1 min, Fig. 2a), the conductivity map reconstructed with the Monte Carlo method (duration: 400 min, Fig. 2b) is distinctly smoother with less severe edge artifacts (black regions in Fig. 2 indicate negative conductivity values). Conductivity in white matter achieved by the Monte Carlo method was 0.50 ± 0.15 S/m, which is in line with literature¹⁴ (0.34 S/m).

DISCUSSION – The proposed Monte Carlo method yielded good signal-to-noise ratio (SNR) and substantially reduced edge artifacts with acceptable computation time. One limitation of the algorithm is the requirement of a sufficiently large number of voxels in each tissue region. In particular, reasonable conductivity values in the bio-physiological range¹⁴ were only obtained in larger tissue regions (white matter in the brain) with both the proposed algorithm and the literature algorithm. This may be explained by insufficient numbers of voxels in smaller tissue regions (gray matter and cerebrospinal fluid in the brain) in the Monte Carlo approach and the predominance of edge artifacts associated with the literature algorithm. Imaging at higher spatial resolution may mitigate this effect in the future. Besides, substantially increased computation time of the Monte Carlo method in the volunteer experiment compared to the phantom experiment may result from the higher complexity of the anatomic structure. High performance computation, e.g. GPU-based computation, may be utilized in the future to reduce the computation time.

CONCLUSION – Reconstruction of conductivity images in the spatial domain with a novel Monte-Carlo-based approach is feasible and substantially decreases the artifact level.

REFERENCES – [1] Kim et al., 2013. *Magn Reson Med*. doi:10.1002/mrm.24759. [2] Katscher et al., 2013. *Comput Math Methods Med*. 2013:546562. [3] van Lier et al., 2013. *ISMRM*. #0115. [4] Goldsmith et al., 1975. *Physiol Chem Phys*. 7:263-9. [5] Schweser et al., 2013. *ISMRM*. #1459. [6] Schweser et al., 2013. *ISMRM*. #2192. [7] Katscher et al., 2012. *ISMRM*. #3842. [8] Canny et al., 1986. *IEEE T Pattern Anal*. 8:679-98. [9] Weisskoff et al., 1992. *Magn Reson Med*. 24:375-83. [10] Herrmann et al., 2013. *ISMRM*. #3239. [11] Zwart et al., 2012. *Magn Reson Med*. 67:701-10. [12] Abdul-Rahman et al., 2007. *Appl Opt*. 46:6623-35. [13] Stogryn et al., 1971. *IEEE T Microw Theory*. 19:733-6. [14] Gabriel et al., 1996. *Phys Med Biol*. 41:2271-93.

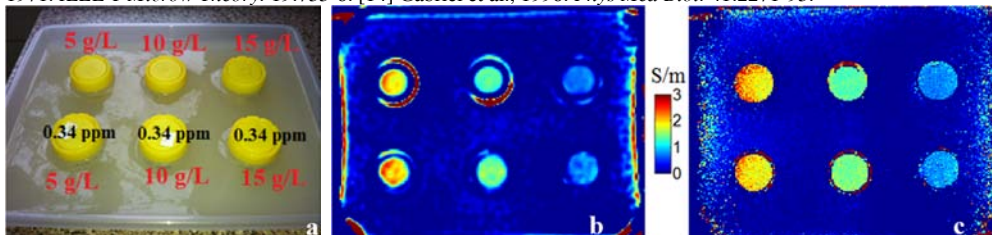


Figure 1. Methods and results of the phantom experiment. Photo of phantom (a). Conductivity maps of the phantom calculated with Gaussian-filtered Laplacian calculus (b) and the novel Monte-Carlo-based method (c). Conductivity values versus saline concentration in the phantom (d).

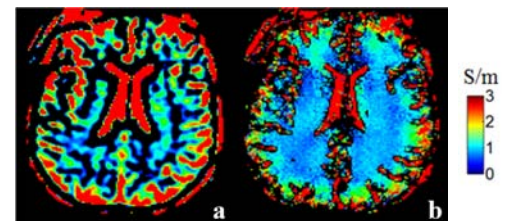


Figure 2. Conductivity maps of the brain calculated with Gaussian-filtered Laplacian calculus (a) and the novel proposed Monte Carlo method (b).

